
Feed-Forward Source-Free Latent Domain Adaptation via Cross-Attention

Ondrej Bohdal¹, Da Li², Shell Xu Hu², Timothy Hospedales^{1,2}

¹ School of Informatics, The University of Edinburgh, UK *

² Samsung AI Center Cambridge, UK

{ondrej.bohdal, t.hospedales}@ed.ac.uk, {da.li1, shell.hu}@samsung.com

Abstract

We study the highly practical but comparatively under-studied problem of latent-domain adaptation, where a source model should be adapted to a target dataset that contains a mixture of unlabelled domain-relevant and domain-irrelevant examples. Furthermore, motivated by the requirements for data privacy and the need for embedded and resource-constrained devices of all kinds to adapt to local data distributions, we focus on the setting of feed-forward source-free domain adaptation, where adaptation should not require access to the source dataset, and also be back propagation-free. Our solution is to meta-learn a network capable of embedding the mixed-relevance target dataset and dynamically adapting inference for target examples using cross-attention. The resulting framework leads to consistent improvement on strong ERM baselines. We also show that our framework sometimes even improves on the upper bound of domain-supervised adaptation, where only domain-relevant instances are provided for adaptation. This suggests that human annotated domain labels may not always be optimal, and raises the possibility of doing better through automated instance selection.

1 Introduction

Domain shift presents a real-world challenge for the application of machine learning models because performance degrades when deployment data are not from the training data distribution. For example, a model that has been only trained on day-time images will perform poorly when presented with night-time images. This issue is ubiquitous as it is often impossible or prohibitively costly to pre-collect and annotate training data that is sufficiently representative of test data statistics. The field of domain adaptation [19, 6] has therefore attracted a lot of attention with the promise of adapting models during deployment to perform well using only unlabeled deployment data.

In this paper we make two main contributions: A conceptual contribution, framing domain adaptation in a new highly practical way; and an algorithm for effective domain adaptation in these conditions.

Latent domain adaptation While domain adaptation is now very well studied [19, 6], the vast majority of work assumes that suitable meta-data is available in order to correctly group instances into one or more subsets (domains) that differ statistically across groups, while being similar within groups. We join a growing minority [27, 7, 13, 34] in arguing that this is an overly restrictive assumption that does not hold in most real applications of interest. On one hand some datasets or collection processes may not provide meta-data suitable for defining domain groupings. Alternatively, for other data sources that occur with rich meta-data there may be no obviously correct grouping and existing domain definitions may be sub-optimal [7]. Consider the popular iWildCam [2] benchmark for animal detection within the WILDS [17] suite. The default setup within WILDS defines domains by camera ID. But given that images span different weather conditions and day/night cycles, such domains may neither be internally homogenous, nor similarly distinct. For example there may be

* Work done during an internship at SAIC

more transferability between images from nearby cameras at similar times of day than between images from the same camera taken on a sunny day vs a snowy night. As remarked by some [13, 34], domains may more naturally define a continuum, rather than discrete groups. And that continuum may even be multi-dimensional – such as timestamp of image and spatial proximity of cameras. In this paper, we propose a flexible formulation of the domain adaptation problem that can span all these situations where domains are hard to define, while aligning with the requirements of real use cases.

Feed-forward and source-free conditions Unsupervised domain adaptation aims to adapt models from source datasets (e.g. ImageNet) to the peculiarities of specific data distributions in the wild. The mainstream line of work uses labelled source domain data alongside unlabelled target domain data and updates the model so it performs well on the target domain using backpropagation [19, 6]. However, the key use cases motivating domain adaptation are edge devices such as autonomous vehicles, smartphones or hospital scanners. Storing and processing large source datasets on such devices is usually infeasible. This has led a growing number of studies to investigate the *source-free* condition [25], where a pre-trained model is distributed and adapted using only unlabeled target data.

In this paper, we go further in considering the practical requirements of an edge device, namely that most edge devices are not designed in either hardware or software stack to support back-propagation. This leads us to focus on the *feed-forward* condition where adaptation algorithms should proceed using only feed-forward operations. For example, simply updating batch normalisation statistics, which can be done without back-propagation, provides a strong baseline for adaptation [29, 36].

Feed-forward source-free latent domain adaptation Bringing these ideas together, we envisage a setup where edge devices maintain an unlabeled target dataset that need not be a cleanly meta-data induced domain in the conventional sense, but which may contain examples relevant to the inference of test instances. Instances in the target set may be of varied relevance to a given test instance. For example, if true instance relevance is a function of timestamp similarity. These target examples should then drive model adaptation on the fly, leveraging neither source data, nor back-propagation.

To solve the challenge posed above, we propose a feed-forward adaptation framework based on cross-attention between test instances and the target set. The cross-attention module is meta-learned based on a set of training domains, inspired by [36]. During deployment it flexibly enables each inference operation to draw upon any part of the target set, exploiting each target instance to a continuous degree. For example, this could potentially exclude transfer from target instances that would be conventionally in-domain (e.g., same camera/opposite time of day example earlier), include transfer from target instances that would conventionally be out-of-domain (e.g., similar images/different camera example earlier), and continuously weight similarity to each target image (e.g., temporal distance of images taken in sequence). Our experiments show that our cross-attention approach provides useful adaptation in this highly practical setting across a variety of synthetic and real benchmarks.

2 Background and related work

Source-free domain adaptation SFDA has emerged as a practical scenario where no source data are available during adaptation and a pre-trained model is adapted to target domain data. [25] were among the first to observe that unsupervised domain adaptation can be done even without access to the source data and proposed a method called SHOT. SHOT utilizes information maximization and self-supervised pseudo-labeling to align target and source domain representations. In fact, most SFDA methods use pseudolabels – soft labels predicted by the pretrained model – as the basis for adapting the model. Further recent approaches include 3C-GAN [23] and NRC [35]. 3C-GAN synthesizes labeled target-style training images based on the conditional GAN to provide supervision for adaptation, while NRC does a neighbor-based update for SFDA that uses RNN for thresholding noisy updates. SFDA has also been applied to semantic segmentation [21, 26] and object detection [15] problems. SFDA in general is regarded as a highly challenging domain adaptation scenario, but as one of high practical value because it does not require access to source data.

Test-time domain adaptation TTDA is related to SFDA and focuses on directly adapting to the specific mini-batch at test time. A meta-learning framework for TTDA has been recently proposed under the name adaptive risk minimization (ARM) [36]. ARM provides a variety of options for how TTDA is done, including context network that embeds information from the whole minibatch, updates to batch normalization statistics and gradient-based fine-tuning on the minibatch. ARM learns to do

TTDA by meta-learning across a large number of tasks. TENT [33] is another TTDA method and is based on optimizing channel-wise affine transformation according to the current minibatch.

Latent domains In settings with latent domains, information about domains is not available i.e. there are no domain labels. Further, some domains may be more similar to each other so the boundaries between domains are often blurred. Various approaches have been proposed to deal with latent domains, e.g. sparse latent adapters [7], domain agnostic learning [28] that disentangles domain-specific features from class information using an autoencoder and [27] that discovers multiple latent domains using a specialized architecture with multiple branches. However, these methods focus on standard domain adaptation or supervised learning that is done across many epochs of training.

Meta-learning Meta-learning can take various forms [14], but one of the most common is episodic meta-learning where the learning is done across tasks. As part of episodic meta-learning, the goal is to learn meta-parameters that will help achieve strong performance when presented with a new task. The most popular application of episodic meta-learning is few-shot learning, where we try to e.g. learn to distinguish between different classes after seeing only a few examples of each class. Example meta-parameters include weight initialization [9, 1, 24] or metric space as is the case in Prototypical networks [30] and RelationNet [31]. Prototypical networks and RelationNet are both examples of feed-forward methods. Episodic meta-learning has also been used in domain generalization [22] and as part of the ARM framework [36]. We also use the episodic meta-learning paradigm.

Transformers As part of our method, we use cross-attention that takes inspiration from the attention mechanism found in the transformer architecture [32]. After transformers became common in natural language processing, they have also led to strong results within computer vision, most prominently as part of the ViT model [8]. ViT model has served as foundation for more recent vision transformers, including CrossViT [4] that combines strong performance with efficiency. Our cross-attention mechanism is broadly inspired by the CrossViT cross-attention module [4]. Our approach has also been inspired by the idea of non-parametric transformers [18] that are able to reason about relationships between data points. Different to CrossViT, we use image-image attention, rather patch-patch, and show how to exploit this for feed-forward source-free latent domain adaptation.

3 Methods

3.1 Set-up

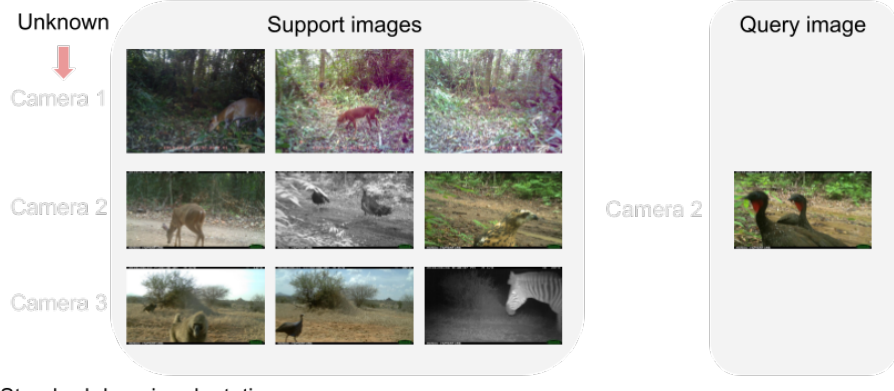
Preliminaries During deployment the high-level assumption made by many source-free domain adaptation frameworks is that we are provided with a predictive model f_ψ and an unlabeled target dataset \mathbf{x}_s whose label-space is the same as that of the pre-trained model [25]. Given these, source-free DA approaches define some algorithm \mathcal{A} that ultimately leads to classifying a test instance x_q as $y_q \approx \hat{y}_q = \mathcal{A}(x_q, \mathbf{x}_s, \psi)$. There are numerous existing algorithms for this. For example, pseudo-label strategies [25, 23, 35] proceed by estimating labels \hat{y}_s for the target set \mathbf{x}_s , treating these as ground-truth, backpropagating to update the model ψ' such that it predicts \hat{y}_s , and then classifying the test point as $f_{\psi'}(x_q)$. We address the *feed-forward* setting where algorithm \mathcal{A} should not use back-propagation. For example, BN-based approaches [29, 36] use the target set \mathbf{x}_s to update the BN statistics in ψ as ψ' and then classify the test point as $f_{\psi'}(x_q)$.

While the conventional domain adaptation setting assumes that x_q and \mathbf{x}_s are all drawn from a common distribution, the *latent domain* assumption has no such requirement. For example, \mathbf{x}_s may be drawn from a mixture distribution and x_q may be drawn from only one component of that mixture. In this case only a subset of elements in \mathbf{x}_s may be relevant to adapting the inference for x_q .

Deployment phase Rather than explicitly updating model parameters, we aim to define a flexible inference routine f_ψ that processes both x_q and \mathbf{x}_s to produce \hat{y}_q in a feed-forward manner, i.e., $\hat{y}_q = \mathcal{A}(x_q, \mathbf{x}_s, \psi) = f_\psi(x_q, \mathbf{x}_s)$. In this regard our inference procedure follows a similar flow to variants of ARM [36], with the following key differences: (1) ARM is transductive: it processes a batch of instances at once without distinguishing test instances and target adaptation set, so elements x_q are members of \mathbf{x}_s . (2) ARM makes the conventional domain-observed assumption that domains have been defined by an external process that ensures all x_q and \mathbf{x}_s are drawn from the same distribution. We do not make this assumption and require robustness to irrelevant elements in \mathbf{x}_s .

Training phase To train a model than can be used as described above, we follow an episodic meta-learning paradigm [36, 14]. This refers to training f_ψ using a set of simulated domain adaptation tasks.

Latent domain adaptation:



Standard domain adaptation:

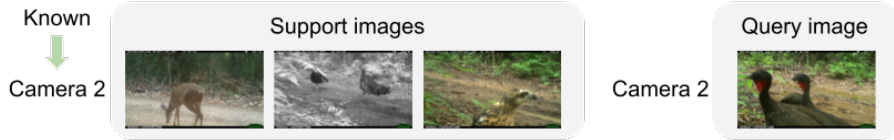


Figure 1: Illustration of how the LDA tasks are structured and how the structure compares to standard DA. In LDA, support images come from a variety of domains and do not have any class or domain labels. The query images come from one of the support domains.

At each iteration, we generate a task with a unique pair of query and support instances $(\mathbf{x}_s, (y_q, x_q))$ keeping label space the same across all tasks. We simulate training episodes where \mathbf{x}_s contains instances with varying relevance to x_q . The goal is for f_ψ to learn how to select and exploit instances from \mathbf{x}_s in order to adapt inference for x_q to better predict y_q .

In particular, our task sampler defines each task as having support examples uniformly sampled across a random set of N_D domains, with the query example being from one of these domains. More formally, each task can be defined as:

$$\mathcal{T} = \{\{x_{s,1}, x_{s,2}, \dots, x_{s,N_s}\}, x_q, y_q\}$$

for N_s unlabelled support examples $x_{s, \cdot}$ and query example x_q with label y_q .

Example We give an example of a task in Figure 1 for $K = 3$ domains with $N_s = 3$ support examples and $N_q = 1$ query example. The chosen example comes from the real-world iWildCam dataset [2], where cameras at different locations are meant to act as different domains. This is challenging, as our model is not provided with this domain/camera annotation in the latent DA setting, and must learn to estimate relevance. On the other hand, we can see from this example that sometimes images from the same annotated domain (= camera) are not very similar, and conversely images from other domains may be quite similar. It may be possible for a model in this setup to do better than standard observed-domain methods that assume an external process provides exclusively same-domain data for adaptation. Our experiments will confirm that this can sometimes happen.

3.2 Objective

Our goal is to train a model that can adapt to relevant examples from the support set and obtain superior performance on the query examples. We can formalize this using the following objective:

$$\min_{\theta, \phi, \omega} \mathcal{E}(\theta, \phi, \omega) = \mathbb{E}_{p_z | \{z_i\}} \left[\mathbb{E}_{p_{\{x_q, y_q | z\}, \{x_s | \{z_i\}\}}} \left[\frac{1}{N_q} \sum_{k=1}^{N_q} \ell(f_\phi(f_{\theta \circ \omega}(x_{q,k}; \mathbf{x}_s), y_{q,k})) \right] \right], \quad (1)$$

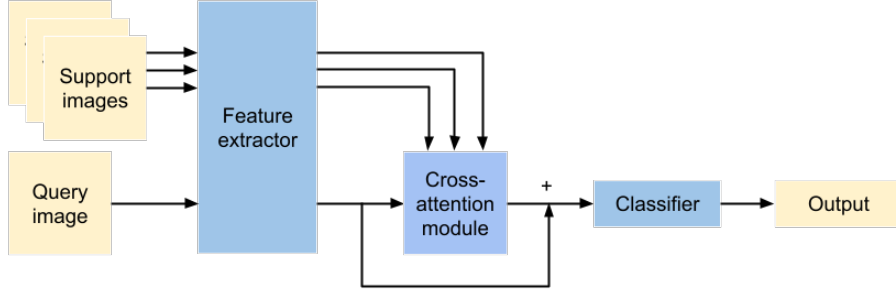


Figure 2: Illustration of how cross-attention is used within the overall architecture.

where $\psi = \{\theta, \phi, \omega\}$ are the parameters of the feature extractor, classifier and cross-attention module respectively (described in detail next), \mathbf{x}_s are the support examples used for adaptation, while \mathbf{x}_q are the query examples for which we make predictions and come from domain z . The support examples come from a set of domains $\{z_i\}$ with $z \in \{z_i\}$. There are N_q query examples and \mathcal{E} represents the generalization error after adapting the model.

3.3 Architecture

The key to solving Eq. 1 is defining an architecture f_ψ that can identify and exploit relevant support instances within \mathbf{x}_s . Our solution to this relies on cross-attention between query and support images, as illustrated in Figure 2. We first embed the support and query examples using the same feature extractor, after which we pass the embeddings through the cross-attention module. The cross-attention module gives us transformed query examples that are then added to the embeddings of the query examples as a residual connection, after which the classifier makes predictions. Compared to CrossViT [4], we do cross-attention between support and query images from different domains, image-to-image rather than patch-to-patch and on extracted features right before the classifier layer.

Cross-attention module Given a set of support examples \mathbf{x}_s and query examples \mathbf{x}_q , we use the feature extractor f_θ to extract features $f_\theta(\mathbf{x}_s), f_\theta(\mathbf{x}_q)$. Cross-attention module $\text{CA}_\omega(f_\theta(\mathbf{x}_s); f_\theta(\mathbf{x}_q))$ parameterized by ω then transforms query embeddings $f_\theta(\mathbf{x}_q)$, using support embeddings $f_\theta(\mathbf{x}_s)$ as keys. The output of the cross-attention module is added to the query example features as a residual connection, which is then used by the classifier f_ϕ to predict labels of the query examples $\hat{y}_q = f_\phi(f_\theta(\mathbf{x}_q) + \text{CA}_\omega(f_\theta(\mathbf{x}_s); f_\theta(\mathbf{x}_q)))$.

The cross-attention module itself performs image-to-image cross-attention, rather than patch-to-patch. More specifically, after extracting the features we flatten all spatial dimensions and channels into one vector, which represents the whole image. Image-to-image attention is more suitable for domain adaptation than patch-based option because the overall representation should better capture the nature of the domain rather than a patch. Another benefit of image-to-image attention is also that it is significantly more efficient – we attend to the whole image rather than patches, which makes the overall computations manageable even with more images.

Our cross-attention module is parameterized by a set of learnable projection matrices $\mathbf{W}_q, \mathbf{W}_k, \mathbf{W}_v$ (all of size $\mathbb{R}^{C \times (C/R)}$) with additional projection matrix $\mathbf{W} \in \mathbb{R}^{(C/R) \times C}$ to transform the queried outputs (we refer to all of these parameters collectively as ω). The output of the feature extractor f_θ is flattened into one vector (any spatial information is flattened), giving C channels, so $f_\theta(\mathbf{x}_q) \in \mathbb{R}^{N_q \times C}, f_\theta(\mathbf{x}_s) \in \mathbb{R}^{N_s \times C}$. We also specify ratio R that allows us to use rectangular projection matrices with fewer parameters, which improves efficiency and also provides regularization.

Formally we express CA_ω as:

$$\mathbf{q} = f_\theta(\mathbf{x}_q)\mathbf{W}_q, \quad \mathbf{k} = f_\theta(\mathbf{x}_s)\mathbf{W}_k, \quad \mathbf{v} = f_\theta(\mathbf{x}_s)\mathbf{W}_v,$$

$$\mathbf{A} = \text{softmax} \left(\mathbf{q}\mathbf{k}^T / \sqrt{C/h} \right), \quad \text{CA}_\omega(f_\theta(\mathbf{x}_s)) = \mathbf{A}\mathbf{v}.$$

Algorithm 1 Episodic meta-learning for source-free latent domain adaptation with CXDA

```
// Meta-training
Require: # training steps  $T$ , # latent domains in a task  $N_D$ , # support examples  $N_s$ , # query examples  $N_q$ , learning rate  $\eta$ 
1: Initialize:  $\theta, \phi, \omega$ 
2: for  $t = 1, \dots, T$  do
3:   Sample  $N_D$  support domains  $\{\mathbb{D}_s\}_1^{N_D}$  from training domains
4:   Sample query domain  $\mathbb{D}_q$  from the set of support domains  $\{\mathbb{D}_s\}_1^{N_D}$ 
5:   Sample  $N_s$  unlabelled support images  $\mathbf{x}_s$  uniformly from the selected support domains  $\{\mathbb{D}_s\}_1^{N_D}$ 
6:   Sample  $N_q$  labelled query images  $\mathbf{x}_q, \mathbf{y}_q$  from domain  $\mathbb{D}_q$ 
7:   Predict query labels  $\hat{\mathbf{y}}_q \leftarrow f_\phi(f_\theta(\mathbf{x}_q) + \text{MCA}_\omega(\text{LN}(f_\theta(\mathbf{x}_s)); \text{LN}(f_\theta(\mathbf{x}_q))))$ 
8:    $(\theta, \phi, \omega) \leftarrow (\theta, \phi, \omega) - \eta \nabla_{(\theta, \phi, \omega)} \sum_{k=1}^{N_q} \ell(\hat{\mathbf{y}}_{q,k}, \mathbf{y}_{q,k})$ 
9: end for
// Inference on a new task
Require:  $\theta, \phi, \omega$ , support  $\mathbf{x}_s$  and query  $\mathbf{x}_q$  examples from new domains
10:  $\hat{\mathbf{y}}_q \leftarrow f_\phi(f_\theta(\mathbf{x}_q) + \text{MCA}_\omega(\text{LN}(f_\theta(\mathbf{x}_s)); \text{LN}(f_\theta(\mathbf{x}_q)), \omega))$ 
```

Similarly as CrossViT [4] and self-attention more broadly, we use multiple heads h , so we refer to it as MCA. We also use layer normalization as is the common practice. The output of MCA is added to the query example embeddings as a residual connection:

$$\mathbf{z} = f_\theta(\mathbf{x}_q) + \text{MCA}_\omega(\text{LN}(f_\theta(\mathbf{x}_s)); \text{LN}(f_\theta(\mathbf{x}_q))),$$

which is then passed through the classifier f_ϕ to obtain predictions $\hat{\mathbf{y}} = f_\phi(\mathbf{z})$. Following CrossViT, we do not apply a feed-forward network after cross-attention. We directly add the output via residual connection and pass it to the classifier.

3.4 Meta-learning

We train the main model (composed of the feature extractor f_θ and classifier f_ϕ and the cross-attention module (parameterized by ω) by meta-learning across many tasks. Each task has the structure described earlier in Section 3.1. Meta-learning is computationally efficient in this case because the inner loop does not include back-propagation based optimization – the adaptation to the support examples is done purely feed-forward. We provide a summary of both how meta-training and inference (meta-testing) is done in Algorithm 1.

4 Experiments

4.1 Benchmarks

We evaluate our approach on a variety of synthetic and real-world benchmarks, namely FEMNIST [3], CIFAR-C [12], TinyImageNet-C [12] and iWildCam [2]. All of these benchmarks have a large number of domains, e.g. around 100 for CIFAR-C and TinyImageNet-C and around 300 for FEMNIST and iWildCam. We provide brief description of each benchmark.

FEMNIST FEMNIST dataset includes images of handwritten letters and digits, and is derived from the EMNIST dataset [5] by treating each writer as a domain.

CIFAR-C CIFAR-C extends CIFAR-10 [20] by applying a variety of corruptions such as different brightness, snow or various types of blurring. There are different levels of severity with which the corruptions are applied, giving rise to multiple domains for the different levels.

TinyImageNet-C Extension of TinyImageNet analogous to CIFAR-C.

iWildCam A large-scale real-world dataset that includes images of different animal species taken by cameras in different locations. There is a lot of variability in the style of images in different cameras, for example different illumination, camera angle or vegetation. The dataset has also substantial class imbalance, so macro F1 score is used for evaluation.

For FEMNIST, CIFAR-C and TinyImageNet-C we follow the splits into meta-training, meta-validation and meta-testing sets from [36]. For iWildCam we follow the splits of domains selected in [17]. Additionally for iWildCam we filter out all domains that have fewer than 40 examples.

4.2 Baselines

ERM Empirical risk minimization or ERM is a baseline that simply trains on all training domains and performs no domain adaptation. It is known to work surprisingly well and is often difficult to beat when properly tuned [10]. In our case it is trained following the episodic pipeline for fair comparison i.e. it is directly trained using the query examples during meta-training.

BN A simple and often useful method for source-free domain adaptation is to update the batch normalization statistics using the unlabelled target domain data [29]. It has achieved strong results in conventional SFDA [16]. However, in the latent DA setting it is unclear if statistics calculated across a support set of varying relevance will be helpful for achieving better performance. During evaluation, the statistics are updated using all support examples, and directly used for the query examples.

CML Contextual Meta-Learning is the main instantiation of ARM [36] as a way to extract information from the whole minibatch in test-time adaptation and use it to obtain better performance on test images. We apply the CML on the whole support set with images from different domains and then use it as additional information for making predictions on test images. CML is a feed-forward domain adaptation method, but it has not been designed for the latent domain adaptation problem.

4.3 Implementation details

Our solution - CXDA Our cross-attention module first flattens all spatial information and channels into one vector for each image, so it works image-to-image. In line with existing literature [32, 4] we use 8 heads and layer normalization on the flattened features of support and query images. The use of layer normalization means that our approach does not rely on a minibatch of query examples i.e. it natively supports streaming mode and does not need multiple query examples to obtain strong results, unlike existing test-time domain adaptation approaches [36, 33].

Support images are projected into keys and values, while query images act as queries for cross-attention after transformation by a projection matrix. After calculating the attention map and applying it to the values, we multiply the output by a further projection matrix. We use only one cross-attention layer and our projection matrices have rectangular shape of $C \times C/2$ where C is the dimensionality of the flattened features. No dropout is used.

Data augmentation We use weak data augmentation during meta-training. The exact augmentations are cropping, horizontal flipping, small rotations (up to 30 degrees) and are different from the corruptions tested in some of the benchmarks. These are applied with probability 0.5 independently.

Task sampling Our tasks have 5 support domains, with 20 examples in each, overall 100 support examples. Query examples come from one randomly selected support set domain (out of 5 options) and there are 20 of them. Note that the method fully supports streaming mode, so no statistics are calculated across the batch and it works independently for each. The exact number of tasks for meta-validation and meta-testing is 420 validation and 420 test for FEMNIST, 850 validation and 11000 test for CIFAR-C, 1700 validation and 11000 test for TinyImageNet-C, and 745 validation and 2125 test tasks for iWildCam.

Training We follow the hyperparameters used in [36] for FEMNIST, CIFAR-C and TinyImageNet-C, and we also train the cross-attention parameters with the same optimizer. For FEMNIST and CIFAR-C a small CNN model is used, while for TinyImageNet-C a pre-trained ResNet-50 [11] is fine-tuned. For iWildCam we follow the hyperparameters selected in [17], but with images resized to 112×112 , training for 50 epochs and with mini-batch size resulting from our task design (100 support and 20 query examples). All our experiments are repeated across three random seeds.

Evaluation metrics We follow [36] in reporting average and worst performance over all testing tasks. While [36] reports the worst single task, we modify this metric to report the average performance of the worst decile of tasks. The reason is that for some benchmarks, among all 10,000+ test tasks with varying domain transfer difficulty there can easily be at least one task with zero accuracy, making it a less meaningful measure.

4.4 Results

We report our results in Table 1 for all benchmarks: FEMNIST, CIFAR-C, TinyImageNet-C and large-scale real-world iWildCam benchmark. We include both average performance as well as reliability via the worst case performance [36], with our bottom decile modification. From the results we can see our cross-attention approach results in consistent improvements over the strong ERM baseline across all benchmarks, as well as the CML and BN baselines. The encouraging result on iWildCam highlights our method works well also in practical real-world scenarios.

Overall we see CML and BN strategies that naively combine information from all support examples have limited success when the support set has both domain relevant and domain irrelevant examples. In fact, CML achieves lower performance than ERM in some of the benchmarks, despite having a mechanism for domain adaptation. The results show the need to adaptively select the right examples from the support set when they come from domains of mixed relevance. We see a confirmation our proposed mechanism based on cross-attention can successfully select useful information from the set of examples with both relevant and irrelevant examples and ultimately achieve superior performance.

Table 1: Main results on synthetic and real-world benchmarks: average and worst-case (worst 10% tasks) test performance, with standard error of the mean across 3 random seeds. Accuracy is reported for all except iWildCam, where F1 score is used (%).

Approach	FEMNIST		CIFAR-C		TinyImageNet-C		iWildCam	
	W10%	Avg	W10%	Avg	W10%	Avg	W10%	Avg
ERM	52.7 \pm 1.4	77.2 \pm 0.9	44.3 \pm 0.5	68.6 \pm 0.3	4.8 \pm 0.2	26.4 \pm 0.4	0.0 \pm 0.0	38.7 \pm 0.8
CML[36]	50.4 \pm 1.3	76.0 \pm 0.9	44.8 \pm 0.5	69.5 \pm 0.5	4.8 \pm 0.5	25.7 \pm 0.6	0.0 \pm 0.0	38.7 \pm 1.1
BN [16, 36]	52.2 \pm 1.5	78.0 \pm 0.7	45.4 \pm 0.7	69.3 \pm 0.4	5.9 \pm 0.2	27.7 \pm 0.3	1.9 \pm 1.1	42.5 \pm 0.8
Our CXDA	53.3 \pm 0.6	78.3 \pm 0.0	49.4 \pm 0.6	72.0 \pm 0.3	6.5 \pm 0.2	28.6 \pm 0.3	3.6 \pm 1.5	43.5 \pm 1.5

4.5 Further analysis

As part of analysis we study several questions: 1) How does the performance of unsupervised cross-attention compare with a supervised version? 2) How does the inference and training time compare for our cross-attention method and the baselines? 3) What do the attention weights look like and what do they imply?

Domain-supervised vs domain-unsupervised adaptation Recall that our main CXDA algorithm and experiments above are domain unsupervised. This may induce a cost due to distraction by domain-irrelevant adaptation data (e.g., as observed by CML underperforming ERM previously) or a potential benefit due to enabling transfer. We therefore compare our unsupervised method with a domain-supervised alternative, with manually defined attention weights based on domain labels. Table 2 shows the results are dataset dependent. The fact that in at least some cases domain-unsupervised adaptation outperforms the supervised case shows that the benefit can sometimes outweigh the cost, and that it is possible for a suitable model to outperform manual domain annotations.

Table 2: Comparison of unsupervised and supervised CXDA on our benchmarks. Average test accuracy for all benchmarks apart from iWildCam where F1 score is reported (%).

Cross-attention	FEMNIST	CIFAR-C	TinyImageNet-C	iWildCam
Unsupervised	78.3 \pm 0.0	72.0 \pm 0.3	28.6 \pm 0.3	43.5 \pm 1.5
Supervised	79.4 \pm 0.4	69.8 \pm 0.4	28.6 \pm 0.2	52.0 \pm 1.2

Comparison of inference and training times We show our approach is fast and can do adaptation quickly in Table 3, with inference time very similar to the baselines. Table 4 shows that meta-training is longer for the smaller datasets, but the difference is small for large datasets and models. All experiments within the same benchmark used the same GPU and number of CPUs.

Analysis of attention weights We have analysed the attention weights to understand the learned behaviour of the cross-attention mechanism. We have selected the large-scale iWildCam benchmark and used one of the trained cross-attention models. Figure 3 shows the density histogram of attention weights for same and different domain support examples, relative to the query examples in each

Table 3: Inference time: average time in ms per task.

Approach	FEMNIST	CIFAR-C	TinyImageNet-C	iWildCam
ERM	12.0 ± 0.1	15.7 ± 0.3	52.8 ± 0.2	352.0 ± 2.8
CML	13.1 ± 0.2	15.8 ± 0.1	48.9 ± 0.1	385.2 ± 8.0
BN	16.5 ± 0.7	19.2 ± 0.2	74.1 ± 0.1	345.2 ± 1.9
CXDA	17.8 ± 1.5	20.5 ± 0.2	77.9 ± 2.8	392.5 ± 1.3

Table 4: Total run time including training: average total running time in minutes.

Approach	FEMNIST	CIFAR-C	TinyImageNet-C	iWildCam
ERM	38.3 ± 0.3	26.6 ± 0.2	94.1 ± 0.2	440.2 ± 5.4
CML	55.2 ± 1.0	35.2 ± 0.2	131.8 ± 0.2	461.9 ± 7.2
BN	44.5 ± 0.3	31.6 ± 0.3	112.3 ± 0.3	432.2 ± 0.8
CXDA	110.0 ± 12.0	63.2 ± 0.6	167.9 ± 1.9	491.6 ± 1.0

task. From the plot we observe that: (i) There is a significant amount of weight spent on attending to examples in different domains to the current query. This suggests that the model is exploiting knowledge transfer beyond the boundaries of the standard (camera-wise) domain annotation in the benchmark, as illustrated in Figure 1. (ii) Nevertheless overall the weight distribution tends to attend somewhat more strongly to the in-domain instances than out-of-domain instances. This shows that our cross-attention module has successfully learned how to match query instances with corresponding domain instances in the support set, despite never experiencing domain-supervision.

4.6 Discussion

Scalability and applicability Our cross-attention approach is fast in the scenario when there are a moderate number of examples for adaptation (in our experiments we use 100), and not too many inferences to be made per adaptation. In this regime it is much faster than the mainstream line of backpropagation-based adaptation solutions [19, 6, 25, 33]. Whereas, if there are very many inferences to be made then the overhead cost of back-propagation would eventually be amortized. As for attention more broadly, its computational cost depends on the number of query and support examples, and the approach would be expensive if there were many thousands or millions of examples for both. For a very large support set, one could simply take a random or semi-random subset of images for adaptation. However, the most cost-effective use case is one where the adaptation set is smaller and/or changes rapidly compared to the frequency of inference.

Broader impact The approach is designed to help obtain better performance in testing settings which are underrepresented in the training data. Hence we expect it to empower underrepresented communities. It is particularly designed to support adaptation in limited amounts of compute, and thus benefit users whose resources may be limited to lower power, embedded or mobile devices.

5 Conclusion

We have introduced a new highly practical setting where we adapt a model using examples that come from a mixture of domains and are without domain or class labels. To answer this new highly challenging adaptation problem, we have developed a novel solution based on cross-attention that is able to automatically select relevant examples and use them for adaptation on the fly.

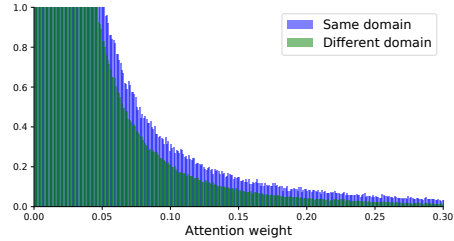


Figure 3: Density histograms of attention weights for pairs of same and different domain examples in the test tasks of iWildCam benchmark.

References

- [1] Antoniou, A., Edwards, H., and Storkey, A. (2019). How to train your MAML. In *ICLR*.
- [2] Beery, S., Cole, E., and Gjoka, A. (2020). The iWildCam 2020 competition dataset. In *arXiv*.
- [3] Caldas, S., Duddu, S. M. K., Wu, P., Li, T., Konečný, J., McMahan, H. B., Smith, V., and Talwalkar, A. (2018). LEAF: A benchmark for federated settings. In *Workshop on Federated Learning for Data Privacy and Confidentiality*.
- [4] Chen, C.-F., Fan, Q., and Panda, R. (2021). CrossViT: Cross-attention multi-scale vision transformer for image classification. In *ICCV*.
- [5] Cohen, G., Afshar, S., Tapson, J., and van Schaik, A. (2017). EMNIST: an extension of MNIST to handwritten letters. In *arXiv*.
- [6] Csurka, G., Hospedales, T. M., Salzmann, M., and Tommasi, T. (2022). Visual domain adaptation in the deep learning era. *Synthesis Lectures on Computer Vision*, 11(1):1–190.
- [7] Deecke, L., Hospedales, T., and Bilen, H. (2022). Visual representation learning over latent domains. In *ICLR*.
- [8] Dosovitskiy, A., Beyer, L., Kolesnikov, A., Weissenborn, D., Zhai, X., Unterthiner, T., Dehghani, M., Minderer, M., Heigold, G., Gelly, S., Uszkoreit, J., and Houlsby, N. (2021). An image is worth 16x16 words: transformers for image recognition at scale. In *ICLR*.
- [9] Finn, C., Abbeel, P., and Levine, S. (2017). Model-agnostic meta-learning for fast adaptation of deep networks. In *ICML*.
- [10] Gulrajani, I. and Lopez-Paz, D. (2020). In search of lost domain generalization. In *arXiv*.
- [11] He, K., Zhang, X., Ren, S., and Sun, J. (2015). Deep residual learning for image recognition. In *CVPR*.
- [12] Hendrycks, D. and Dietterich, T. (2019). Benchmarking neural network robustness to common corruptions and perturbations. In *ICLR*.
- [13] Hoffman, J., Darrell, T., and Saenko, K. (2014). Continuous manifold based adaptation for evolving visual domains. In *CVPR*.
- [14] Hospedales, T. M., Antoniou, A., Micaelli, P., and Storkey, A. J. (2021). Meta-learning in neural networks: a survey. *IEEE Transactions on Pattern Analysis and Machine Intelligence*, PP:1–1.
- [15] Huang, J., Guan, D., Xiao, A., and Lu, S. (2021). Model adaptation: historical contrastive learning for unsupervised domain adaptation without source data. In *NeurIPS*.
- [16] Ishii, M. and Sugiyama, M. (2021). Source-free domain adaptation via distributional alignment by matching batch normalization statistics. In *arXiv*.
- [17] Koh, P. W., Sagawa, S., Marklund, H., Xie, S. M., Zhang, M., Balsubramani, A., Hu, W., Yasunaga, M., Phillips, R. L., Gao, I., Lee, T., David, E., Stavness, I., Guo, W., Earnshaw, B., Haque, I., Beery, S. M., Leskovec, J., Kundaje, A., Pierson, E., Levine, S., Finn, C., and Liang, P. (2021). Wilds: A benchmark of in-the-wild distribution shifts. In *ICML*.
- [18] Kossen, J., Band, N., Lyle, C., Gomez, A. N., Rainforth, T., and Gal, Y. (2021). Self-attention between datapoints: Going beyond individual input-output pairs in deep learning. In *NeurIPS*.
- [19] Kouw, W. M. and Loog, M. (2021). A review of domain adaptation without target labels. *IEEE Transactions on Pattern Analysis and Machine Intelligence*, 43(3):766–785.
- [20] Krizhevsky, A. (2009). Learning multiple layers of features from tiny images. Technical report.
- [21] Kundu, J. N., Kulkarni, A., Singh, A., Jampani, V., and Babu, R. V. (2021). Generalize then adapt: source-free domain adaptive semantic segmentation. In *ICCV*.

- [22] Li, D., Zhang, J., Yang, Y., Liu, C., Song, Y.-Z., and Hospedales, T. M. (2019). Episodic training for domain generalization. In *ICCV*.
- [23] Li, R., Jiao, Q., Cao, W., Wong, H.-S., and Wu, S. (2020). Model adaptation: unsupervised domain adaptation without source data. In *CVPR*.
- [24] Li, Z., Zhou, F., Chen, F., and Li, H. (2017). Meta-SGD: learning to learn quickly for few-shot learning. In *arXiv*.
- [25] Liang, J., Hu, D., and Feng, J. (2020). Do we really need to access the source data? Source hypothesis transfer for unsupervised domain adaptation. In *ICML*.
- [26] Liu, Y., Zhang, W., and Wang, J. (2021). Source-free domain adaptation for semantic segmentation. In *CVPR*.
- [27] Mancini, M., Porzi, L., Bulo, S. R., Caputo, B., and Ricci, E. (2021). Inferring latent domains for unsupervised deep domain adaptation. *TPAMI*, 43(2):485–498.
- [28] Peng, X., Huang, Z., Sun, X., and Saenko, K. (2019). Domain agnostic learning with disentangled representations. In *ICML*.
- [29] Schneider, S., Rusak, E., Eck, L., Bringmann, O., Brendel, W., and Bethge, M. (2020). Improving robustness against common corruptions by covariate shift adaptation. In *NeurIPS*.
- [30] Snell, J., Swersky, K., and Zemel, R. S. (2017). Prototypical networks for few-shot learning. In *NIPS*.
- [31] Sung, F., Yang, Y., Zhang, L., Xiang, T., Torr, P. H., and Hospedales, T. M. (2018). Learning to compare: relation network for few-shot learning. In *CVPR*.
- [32] Vaswani, A., Shazeer, N., Parmar, N., Uszkoreit, J., Jones, L., Gomez, A. N., Kaiser, L., and Polosukhin, I. (2017). Attention is all you need. In *NeurIPS*.
- [33] Wang, D., Shelhamer, E., Liu, S., Olshausen, B., and Darrell, T. (2021). Tent: Fully test-time adaptation by entropy minimization. In *ICLR*.
- [34] Wang, Q., Fink, O., Van Gool, L., and Dai, D. (2022). Continual test-time domain adaptation. In *CVPR*.
- [35] Yang, S., Wang, Y., van de Weijer, J., Herranz, L., and Jui, S. (2021). Exploiting the intrinsic neighborhood structure for source-free domain adaptation. In *NeurIPS*.
- [36] Zhang, M., Marklund, H., Dhawan, N., Gupta, A., Levine, S., and Finn, C. (2021). Adaptive risk minimization: learning to adapt to domain shift. In *NeurIPS*.

A Qualitative analysis

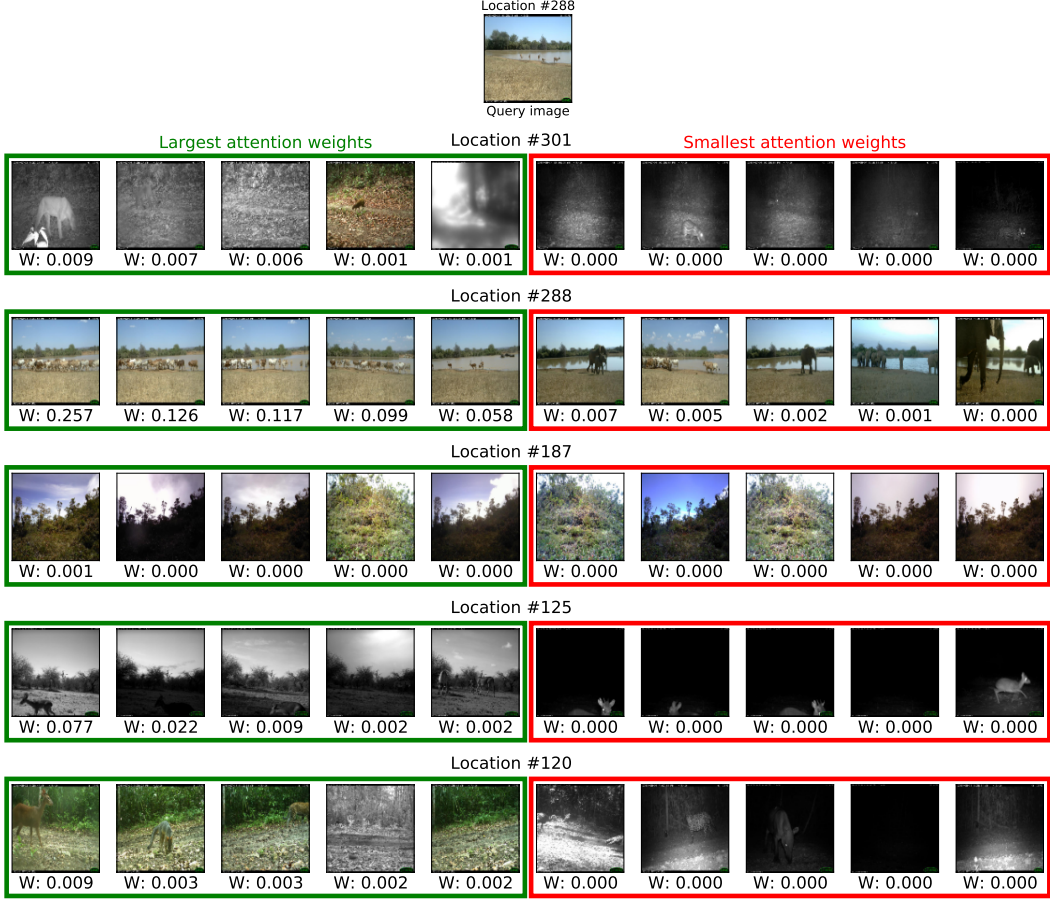


Figure 4: Analysis of attention weights for an example task in iWildCam, with a query image coming from location (camera trap) #288. We show the five support examples in each domain that have the largest and smallest attention weights. Similar images from the same location (#288) are given the largest weights, but also relevant images from other locations (e.g. #125) are given larger weights. The examples with the smallest attention weights visually do not seem relevant.

B Additional details

We have followed the experimental choices from [36] for FEMNIST, CIFAR-10-C, TinyImageNet-C and [17] for iWildCam, unless we specify otherwise. This includes the splits of data into training, validation and test sets as well as the splits of domains into meta-training, meta-validation and meta-test sets of domains. For iWildCam we use the OOD splits from [17].

B.1 Models

Feature extractor and classifier:

- FEMNIST: CNN with three convolutional layers, hidden dimension of 128, batch normalization, ReLU activation, kernel of 5, padding of 2. Classifier consists of two fully-connected layers with 200 hidden units and ReLU activation in between. The input shape of images is 28×28 .
- CIFAR-C: Same architecture as for FEMNIST, but with three input channels instead of 1 (colour images). The input shape of images is 32×32 .

- TinyImageNet-C: ImageNet pre-trained ResNet50 [11]. The classifier consists of one fully connected layer. The input shape of images is 64×64 .
- iWildCam: ImageNet pre-trained ResNet50 [11]. The classifier consists of one fully connected layer. The input shape of images is 112×112 .

Adaptation-specific components:

- CML: Context network is used to transform the support examples – three convolutional layers, 64 hidden units, kernel size of 5, padding of 2, with batch normalization and ReLU activation. The output of the network has the same shape as input. To create the context we average the context network outputs across the support examples and use the same context for all query examples in the task.
- CXDA: All key details are explained in the main text, and we provide more detailed explanations here. The size of the fully-connected layers depends on the flattened shape of the features – only one cross-attention layer is used. After multiplying attention weights with projected values (\mathbf{Av}), we transform the output further using projection matrix \mathbf{W} , similarly as [4]. However, we do not use a further MLP model that would contain multiple layers and non-linearity, so we also follow [4] in this aspect. The output of the cross-attention module has the same shape as input. As part of CXDA, batch normalization statistics of the feature extractor are updated too using the support set.

B.2 Training

Dataset-specific training details:

- FEMNIST: SGD with learning rate of 10^{-4} , momentum of 0.9 and weight decay of 10^{-4} , trained for 200 epochs, with validation set evaluated every 10 epochs, and early stopping based on accuracy.
- CIFAR-C: SGD with learning rate of 10^{-2} , momentum of 0.9 and weight decay of 10^{-4} , trained for 100 epochs, with validation set evaluated every 10 epochs, and early stopping based on accuracy.
- TinyImageNet-C: SGD with learning rate of 10^{-2} , momentum of 0.9 and weight decay of 10^{-4} , trained for 50 epochs, with validation set evaluated every 5 epochs, and early stopping based on accuracy.
- iWildCam: Adam with learning rate of 3×10^{-5} , no weight decay, trained for 50 epochs, with validation set evaluated every 5 epochs, and early stopping based on macro F1 score.

In all cases we use cross-entropy loss, and the cross-attention parameters are optimized in the same way as the main model. In each iteration we use a task that has 5 domains with 20 support examples for each sampled domain, and there are 20 query examples from one selected domain from the set of current domains.

C Computational resources

We have used an internal cluster with NVIDIA GPUs – each experiment used one GPU.

D Licences of assets

All datasets that we use are publicly available. We have extended the official code from [36] (ARM), [4] (CrossViT) and [17] (WILDS - iWildCam), all of which are publicly available on GitHub.